Iranian Journal of Medical Physics

ijmp.mums.ac.ir

# A New Method for Detecting Sperms in Microscopy Images: Combination of Zernike Moments and Spatial Processing

Reza Arkanfari[1], Seyed Vahab Shojaedini[2*]

1. Faculty of Electrical, Biomedical and Mechatronics Engineering, Qazvin Branch, Islamic Azad University, Qazvin, Iran
2. Department of Biomedical Engineering, Iranian Research Organization for Science and Technology, Tehran, Iran.

**ARTICLE INFO**

***Article type:***
Original Article

***Article history:***
Received: Nov18, 2017
Accepted: Apr 05, 2018

***Keywords:***
Infertility
Sperm
Detection
Microscopic Image
Semen
Spatial Processing

**ABSTRACT**

***Introduction***: In recent years, modern microscopic imaging in parallel with digital image processing techniques, have facilitated computerized semen analysis. However, in these methods, distinguishing sperms from other semen particles can be hampered by low contrast of microscopic images and the possibility of neighboring sperms touching each other.

***Materials and Methods:*** This article introduced a new method based on combination of Zernike moments and spatial processing in sperm detection. In the first step, Zernike moments were estimated due to their rotation and noise-resistant nature to mark pixels with some chance of belonging to sperms. In the second step, pruning was executed considering the connectivity of candidates and using morphological processing, to extract sperms. The proposed algorithm was examined on microscopic images exhibiting several sperms with different morphologies.

***Results:*** The obtained results showed the ability of the proposed method in sperm detection, such that it could detect 85% of the sperms without any false detection. In a more pragmatic situation, where false detection rate was 5%, the detection rate of the proposed algorithm increased to 94%.

***Conclusion:*** Comparing the proposed method with watershed segmentation algorithm (WSA) and morphological contour synthesis (MCS) revealed the superiority of the proposed method to its alternatives in such a way that it detected sperms at least 3% and 13% better than WSA and MCS, respectively, without any false detection. Furthermore, the rate of false detections in the proposed algorithm was at least 4% and 14% better than its alternatives.

►*Please cite this article as:*
Arkanfari R, Shojaedini SV. A New Method for Detecting Sperms in Microscopy Images: Combination of Zernike Moments and Spatial Processing. Iran J Med Phys 2018; 15: 215-221. 10.22038/ijmp.2018.27427.1288.

## Introduction

Infertility is a clinical problem, which is defined as not being able to conceive after a year of regular sexual intercourse [1]. The source of almost half of infertilities is male factor [2]. Sperm morphology assessment is the cornerstone of semen analysis. In this process, several effective sperm parameters, including count, shape, and size, are determined. Based on the mentioned parameters, the percentages of normal and abnormal sperms can be calculated, which may be used as a reliable determinant of sperm function or dysfunction according to the World Health Organization 2010 standard for the analysis of human semen [3].

Distinguishing sperms from other parts of semen has become the most challenging issue in semen analysis [4, 5]. Manual sperm detection is often performed in laboratories by an expert andrologist. This outcome of this method is highly affected by experience of the technician, measurement procedure, and human error. Numerous studies have been carried out for the automated sperm detection [6]. In some studies, detection schemes that were based on split-merge concept have been applied on microscopic images to identify sperms. The performances of these methods depend on distances between sperms. Consequently, these methods lead to significant errors in high-density samples, where sperms are located in close proximity [7].

Microscopy images are intrinsically low contrast; therefore, edge detection is not a suitable approach for distinguishing sperms from other parts of semen in these images. Active contour has been widely used in many object detection applications. However, extracting correct contours requires extensive computation. This renders contour-based algorithms very slow and unsuitable for pragmatic situations. Thresholding is another well-known solution for object detection. Although this strategy has low computational complexity, the performance of threshold-based methods is highly sensitive to threshold values. In other words, slight errors in selecting the optimal threshold may lead to either significant lack of sperms or increased false detections [8].

Some studies have used the algorithms that are based on region growing concept to separate sperms from the other parts contained in microscopic images. However, these methods often merge the adjacent

*Corresponding Author: Department of Biomedical Engineering, Iranian Research Organization for Science and Technology, Tehran, Iran. Tel: +982156276311; Email: shojadini@irost.ir

sperms [9]. Some other methods make use of several parameters consisting head area, perimeter, head length, head width, tail length, orientation, and eccentricity to detect sperms [10]. The values of above parameters are obtained empirically to prevent the detection of distorted and agglutinated sperms. Although the existing algorithms have had several breakthroughs in sperm detection, they still have some drawbacks that are summarized below.

i. Distorted sperms may not be detected because of changing their shapes from ellipse, which has been considered as the standard template in several methods.

ii. Agglutination of two or more sperms may not be distinguished because of unexpected combination.

iii. A large number of existing methods are sensitive to noise. In the worst case, image noise is misidentified as the sperm head.

iv. Several methods are not completely automated and they require human intervention to initiate the sperm detection procedure.

Some other methods utilize texture-based descriptors for sperm detection, especially for detecting abnormalities of the head [11]. Furthermore, adaptive mixture models (AMM) and Markov random field (MRF) have been used for segmentation of the head. Artifacts and debris in images affect the performance of such methods, which will be a source of error [12]. Segmentation of the human sperm has also been performed based on clustering methods [13]. Some other methods use concatenation of several geometric steps, which finally leads to ellipse matching. To improve detection procedure, these methods generally strive to eliminate unwanted objects whose shape differs from sperms [14]. In some studies, combinations of principal component analysis (PCA) and clustering methods (e.g., k-nearest neighbor algorithm) have been used to identify sperms [15]. Other feature extraction methods, such as scale-invariant feature transform (SIFT), have also been examined to enhance the detection rate of sperms in microscopic images [15, 16]. Artificial neural networks have also been employed to improve the accuracy of sperm detection in some other works. However, the performance of this method seriously depends on the training set of neural networks, which may impede its effectiveness in real applications [17].

**Prior Studies by Authors**

In [18], a method was introduced for distinguish sperms from other semen particles, which was based on the mapping of wavelet coefficients. In the proposed method, the captured frames were transformed into wavelet sub-bands, and then the bit-related planes were constructed. The above-mentioned bit planes were mapped by different local monograph functions, which led to dividing the image into sperm or non-sperm regions.

In another research [19], authors introduced a new method for sperm detection, which was based on the fuzzy decision concept. In the proposed method, fuzzy rules were applied to select correct sperms and reject false candidates.

The watershed-based segmentation modified by the fuzzy entropy concept was introduced in another article [20] for sperm detection. This method used watershed-based segmentation to select some primary "candidates" to be sperms. Then, the fuzzy entropy decision was applied to confirm correct sperms and reject false ones.

In [21], authors used minimization of the information distance to separate sperms and background. In this method, the co-occurrence matrix was calculated as the indicator of frequency distribution of gray level transition. By using the elements of this matrix, the entropies of transitions over boundaries of image contents were calculated, which indicated some image regions as sperms.

In another research [22], authors used the graph theory to improve sperm detection. In this method, firstly probable sperms were extracted by using segmentation. Then, these particles were pruned during successive frames by using the graph theory concept. Finally, a Kalman filter-based algorithm was applied to confirm the correct sperms. The use of graph theory based on pruning algorithm and Kalman filtering led to the reduction of false detections and provided more valid motility trajectories.

Authors also used morphologic contour for detecting sperms in another research [23]. In the proposed method, sperms were firstly estimated based on their morphologies. In the next step, the energy minimization concept was applied to determine the sperm boundaries.

In their recent work [24], authors proposed a new spatiotemporal processing scheme to distinguish sperms from other contents of semen in microscopy images. In this scheme, the concept of stochastic process was utilized to model sperm behaviors (i.e., histories of sperms). Finally, the cross-correntropies of the constructed models (i.e., stochastic processes) were estimated as a criterion for separating sperms from other parts of semen specimen.

In this paper, a new method is introduced for detecting sperms in microscopy images, which is based on the estimation of Zernike moments followed by spatial processing. The proposed method includes two steps. In the first step, Zernike moments are estimated to select candidate pixels belonging to sperm cells. In the second step, the correct sperms are confirmed by using the connectivity concept and morphological operations. The proposed method has a considerable ability to address the physical limitations of microscopic images because of rotation and noise-resistant nature of Zernike moments.

## Materials and Methods

Firstly, we introduce $I$ as a microscopy image recorded from a semen specimen. Naturally, such an image may contain sperms and several artifacts (i.e., plasma and debris). Each pixel of $I$ may be illustrated as:

$$I_{lj} = I(l, j)$$
$$1 \le l \le L \quad , \quad 1 \le j \le J \tag{1}$$

where $I_{lj}$ represents the intensity of each pixel in the microscopy image. $l$ and $j$ denote the location of the above pixel. Hypothesis testing framework illustrates the dependence of each pixel to either artifact or a sperm as described below:

$$\begin{cases} H_0 : & I_{lj} = \left| a_{lj} + n_{lj} \right| \\ H_1 : & I_{lj} = \left| s_{lj} + a_{lj} + n_{lj} \right| \end{cases} \tag{2}$$

where $s_{lj}$ and $a_{lj}$ represent the sperm and artifact, respectively. $n_{lj}$ Shows the noise component in $I_{lj}$. To determine the dependence of $I_{lj}$ to each of the above hypotheses, $W_{lj}$ signifies a window centered at $(l, j)$, which equals $K_1 \times K_2$ in size. The Zernike moment of order *q* with repetition *m* may be estimated across $W_{lj}$ by using the following equation:

$$(A_{qm})_{lj} = \frac{q+1}{\pi} \sum_{l'=1}^{K_1} \sum_{j'=1}^{K_2} I_{l'j'} \overline{V}_{qm}(\rho, \theta) \tag{3}$$

where $(A_{qm})_{lj}$ shows the Zerninke moment estimated for a window centered at $(l, j)$, in which $V_{qm}(\rho, \theta)$ is illustrated as:

$$V_{qm}(\rho, \theta) = R_{qm}(\rho) e^{im\theta} \tag{4}$$

where $\rho$ and $\theta$ are polar coordinates of the pixel located at $(l', j')$, which are defined as:

$$\rho = \sqrt{l'^2 + j'^2} \quad , \quad \theta = \arctan\left( j' / l' \right) \tag{5}$$

Further, $q$ is a non-negative integer and *m* is an integer number subject to the following constraints:

$$q - |m| = even \quad , \quad |m| \le q \tag{6}$$

$R_{qm}(\rho)$ in Equation (4) is called radical polynomial and is computed as:

$$R_{qm}(\rho) = \sum_{s=0}^{\frac{q-|m|}{2}} \frac{(-1)^s (q-s)! \rho^{q-2s}}{s! \left(\frac{q+|m|}{2} - s\right)! \left(\frac{q-|m|}{2} - s\right)!} \tag{7}$$

where $s$ represents the variable of radial polynomials.

Sliding $W_{lj}$ on all the pixels of $I$ followed by computing their Zernike moments leads to a complex feature space as:

$$A = [(A_{qm})_{lj}] \ , \ 1 \le l \le L \quad , \ 1 \le j \le J \tag{8}$$

Applying Equation (9) leads to determining those pixels that have some chance to be a part of a sperm (i.e., candidates), which creates the pseudo-image *I'*.

$$\begin{cases} I'_{lj} = I_{lj} & \left[ \left| A_{qm} \right|_{lj} \right] \ge \eta \\ 0 & otherwise \end{cases} \tag{9}$$

In the next step, spatial processing is applied to the pseudo-image $I'$ to extract correct sperms. For this purpose, firstly the $D$ connected objects are extracted using a method proposed by Shapiro [25] as mentioned in Equation (9):

$$O = \{O_1, O_2, ..., O_d, ..., O_D\} \tag{10}$$

Then, the members of $O$ are pruned by using three consecutive morphological operations of dilation, filling, and erosion, respectively. Concatenation firstly enlarges the detected candidates by using dilation. Then, the holes are filled, and finally, the boundaries of regions containing sperm candidates are eroded away by using erosion. Based on the above morphologic procedure, the connected objects are reduced to:

$$O' = \{O'_1, O'_2, ..., O'_f, ..., O'_F\} \quad , \quad F \le D \tag{11}$$

By combining equations (2) and (11), dependence of each pixel to artifacts and noise ($H_0$) or to a sperm ($H_1$) is determined as:

$$\begin{cases} H_0 : I_{lj} \notin O'_f \ \Rightarrow I_{lj} = \left| a_{lj} + n_{lj} \right| \\ H_1 : I_{lj} \in O'_f \ \Rightarrow I_{lj} = \left| s_{lj} + a_{lj} + n_{lj} \right| \end{cases} \tag{12}$$

The pseudo-code of the entire detection procedure is presented below, which includes candidate selection, connectivity check, and pruning:

Begin
/* Step 1: compute Zernike moment
1. Move the window as a mask $W_{lj}$ with size $K_1 \times K_2$ on image $I_{lj}$ to sweep all of the pixels and calculate its $(A_{qm})_{lj}$ by Eq. (3).
/* Step2: Extract matrix A
2. The next step after calculate $(A_{qm})_{lj}$ saved in matrix by Eq. (8).
/* Step 3: Detection of candidates
3. Detection of candidate pixels from matrix *A* using Eq. (9).
4. Performing candidate objects by using Eq. (10). the border with white pixels leads to
/* Step 4: Application of morphological operations
5. Applying dilation
6. Applying filling
7. Applying Erosion
/* Step 5: Detection of sperms
8. Finalizing the detecting of sperms by Eq. (12).
End

## Results

The proposed algorithm was applied on various videos obtained from semen microscopy. The data set was captured by an Orca ER Digital CCD Camera mounted on a Nikon invert microscope using a 40x zoom lens. Data set specifications are presented in Table 1. The proposed method was implemented using MATLAB 2016a along with Watershed segmentation algorithm (WSA) [22] and morphological contour synthesis (MCS) [23] to be compared with one another. The captured videos were first processed manually by an expert to obtain a ground truth to compare the automatic methods with. Then, sperms were detected by applying the proposed method and its two alternatives. Finally, the performance of each algorithm was determined by comparing its results with manual detection results.

Two samples of the examined images are exhibited in Figure 1. Figures 2-4 demonstrate the performance of the proposed WSA and MCS methods on those samples. Figure 2-a shows that the proposed method has extracted 34 of the 34 sperms that are presented in Figure 1-a with eight false detections. In a similar manner, Figure 2-b displays that the proposed method has extracted 40 of 42 sperms that are shown in Figure 1-b with six false detections.

Figures 3-a and 3-b show that WSA has extracted 31 and 37 sperms correctly from the reference images 1-a and 1-b, respectively, with 12 and 8 false detections, respectively.

Figure 4-a demonstrates that the other alternative algorithm (i.e., MCS) extracted 31 sperms correctly from the reference image (1-a). Similarly, Figure 4-b demonstrates that this algorithm has extracted only 39 sperms correctly from the image (1-b). These detections were obtained along with 11 and 8 false detections, respectively. These results indicate that the proposed method has a high ability to detect sperms and reject non-sperm objects as follows. For example, in Figure 1-a**,** two non-sperm particles are marked as "1" and "3", further "2" shows a low contrast sperm. Figure 2-a demonstrates that the proposed algorithm also rejects both of these particles, whereas the alternative methods (i.e., WSA and MCS) have considered both of them as sperms, as have been marked in figures 3-a and 4-a.

Object "2" was detected as a correct sperm by the proposed and MCS algorithms as shown in figures 2-a and 4-a, whereas it was overlooked by WSA as shown in Figure 3-a. Other examples can be studied in figures 1-b to 4-b. Figure 1-b displays sperms marked as "2" and "3", as well as non-sperm object "1". Figure 2-b shows that "2" and "3" have been detected and "1" has been rejected correctly by using the proposed scheme. Figure 3-b shows that WSA has yielded completely wrong results about these three marked objects, that is, it has considered "1" as sperm and rejected both "2" and "3". Finally, the results of MCS were a bit more satisfactory since it has correctly considered "2" and "3" as sperms, but it has falsely detected "1" as sperm as shown in Figure 4-b.

**Table 1.** Specifications of test images

| Value | Specification | Value | Specification |
|---|---|---|---|
| Sperm size | 30-50 pixels | Number of frames | 3480 |
| Frame size | 480×720 pixels | Speed of sperms | 0-2 pixel per frames |
| Video frame rate | 29 fps | Average contrast | 23 |
| Number of persons | 11 persons | Density of sperm per milliliter | $> 2\times10^6$ |
| Number of videos | 11 | Age of examined persons | 22-35 years old |

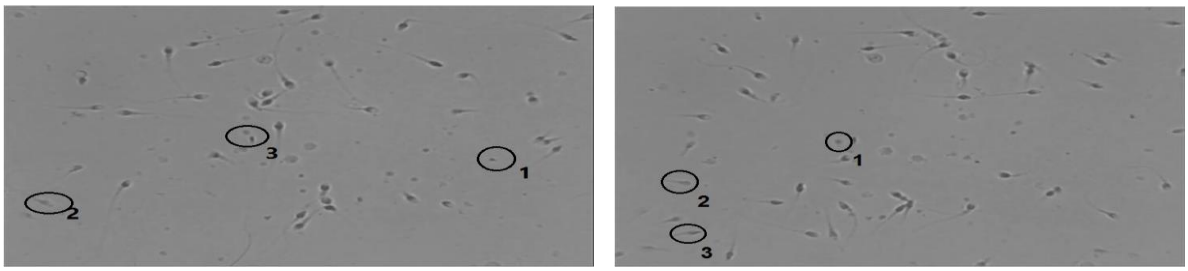


(a) (b)

**Figure 1.** Two captured microscopic images from semen specimens

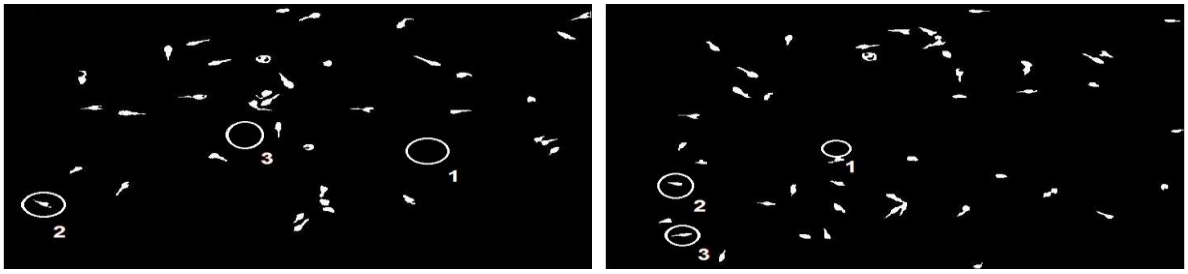

(a) (b)

**Figure 2.** Extracted sperms by using the proposed method

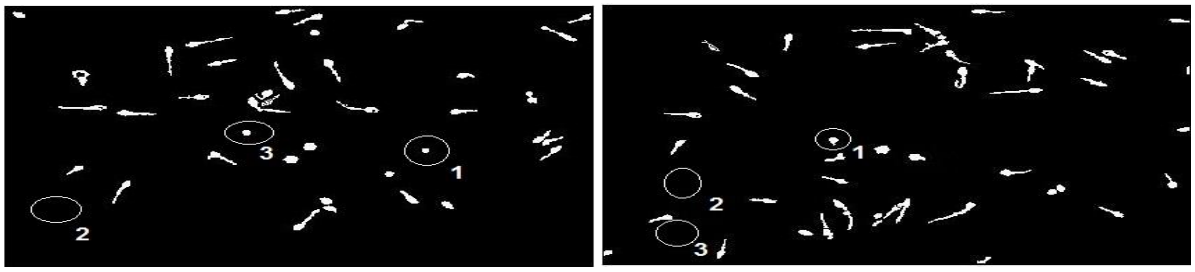

(a) (b)

**Figure 3.** Extracted sperms by using the Watershed segmentation algorithm

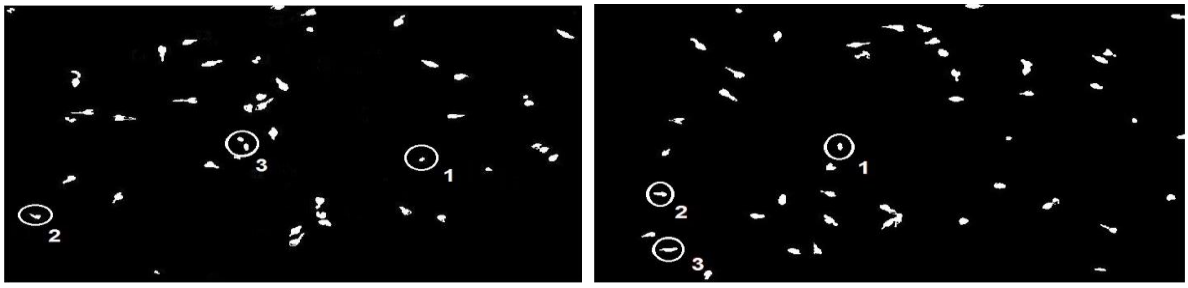

(a) (b)

**Figure 4.** Extracted sperms by using the morphological contour synthesis method

## Discussion

The real data obtained from semen microscopy were analyzed. The proposed algorithm, as well as the WSA and MCS methods, was applied on the data and the results were compared by using the two standard parameters described in equations (13-14), where SR represents the output image by using automatic methods and GT denotes output image of expert analysis. In these images, the pixels belonging to the sperm are labelled as "1" and those belonging to other components are shown by "0". The first parameter is true positive rate (TPR), which demonstrates those pixels that were considered as sperms in both $SR$ and $GT$ images. This parameter has been illustrated by using Equation (13) as:

$$TPR\,(SR,GT\,)=\frac{\#(SR\ \mathrm{I}\ GT\,)}{\#(GT\,)} \qquad (13)$$

Another parameter that is shown in Equation (14) is false positive rate (FPR), which describes those pixels that have been labeled as sperms contrary to expert diagnosis.

$$FPR\,(SR,GT\,)=\frac{\#\left(SR\ \mathrm{I}\ \overline{GT}\right)}{\#(GT\,)} \qquad (14)$$

By using the above parameters, ROC curves were obtained for the three investigated methods. Figure 5 shows changes in TPR versus FPR. These curves indicate that the proposed method outperformed the two alternatives. For better interpretation of ROC results, $FPR=0\%$ and $TPR=100\%$ were considered as ideal values for false and true detections, and Table 2 was constructed using extremes of curve 5. It is obvious in Table 2 that in $FPR=0\%$ the proposed algorithm has shown 3% and 13% superiority to the WSA and MCS algorithms, respectively. At another extreme (i.e., $TPR=100\%$), the proposed algorithm showed 4% and 14% superiority to the WSA and MCS algorithms, respectively.

In addition, the performance of the algorithm was analyzed in $FPR=5\%$ and $TPR=90\%$ as more practical situations in Table 2. For instance, in $FPR=5\%$, the proposed algorithm showed 9% and 4% superiority to WSA and MCS algorithms, respectively, while in $TPR=90\%$, these superiorities were 8% and 4%, respectively.

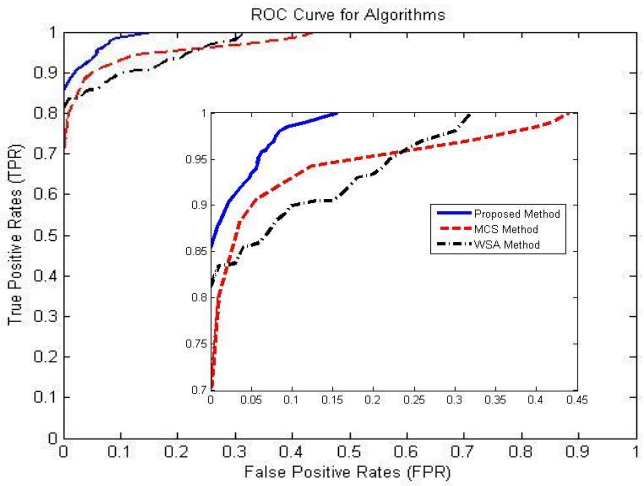


**Figure 5.** Receiver operating characteristic curves obtained for the examined algorithms

**Table 2.** Comparison of performance of the algorithms

| Parameter | Examined algorithms (%) | | |
|---|---|---|---|
| | Proposed | WSA | MCS |
| Detection rate against 0% false alarm | 85 | 82 | 72 |
| False detection rate against 100% detection | 14 | 18 | 28 |
| Detection rate against 5% false alarm | 94 | 85 | 90 |
| False detection rate against 90% detection | 2 | 10 | 6 |
| Area under a curve | 0.4419 | 0.4247 | 0.4225 |

WSA: Watershed segmentation algorithm
MCS: morphological contour synthesis

The performance of algorithms can be compared using other arbitrary thresholds for acceptable FPR and TPR parameters in the same manner.

Another important parameter that is frequently used for comparing detection methods in literature is area under a curve (AUC) [26]. Therefore, this criterion has been used to compare the proposed method to the WSA and MCS methods as shown in Table 2. This comparison showed 2% superiority of the proposed algorithm in sperm detection to its alternatives.

## Conclusion

In this study, a new method was introduced for sperm detection in microscopic images captured from human semen. The proposed algorithm used the concept of Zernike moments to overcome some challenges in distinguishing sperm from other semen parts. To evaluate the performance of the proposed algorithm, it was examined on real microscopic images in conjunction with two other existing methods (i.e., WSA and MCS). Then, the obtained results were compared based on their TPR and FPR. The comparisons showed the superiority of the proposed method to its alternatives. Results showed that the proposed algorithm distinguished sperms from other semen parts at least 9% and 4% better than the other methods in the presence of a typically low FPR (5%). Furthermore, it was shown that the FPR of the proposed algorithm was at least 8% and 4% better than WSA and MCS methods considering the minimum acceptable TPR of 90%. It can be concluded that the proposed method can be used as a suitable choice for detecting sperms in microscopic images captured from human semen.

## Acknowledgment

This article was extracted from a Master's thesis submitted to Islamic Azad University of Qazvin. We wish to thank all those who support us in providing this article. Furthermore, we would like to thank Dr Vahid Reza Nafisi for his valuable encouragement and support.

## References

1. Domar A.D, Broome A, Zuttermeister PC, Seibel M , Friedman R . The prevalence and predictability of depression in infertile women. Fertility and Sterility. 1992; (58) : 1158-63.
2. Maduro M.R, Lamb D.J. Understanding new genetics of male infertility. The Journal of Urology. 2002; 168(5): 2197-205.
3. Franken D.R. How accurate is sperm morphology as an indicator of sperm function? Andrologia. 2014; 47(6): 720-3.
4. Oku H, Ishikawa M, Ogawa N, Shiba , Yoshida M. How to track spermatozoa using high-speed visual feedback. 30th Annual International Conference of

the IEEE Engineering in Medicine and Biology Society. 2008; 125-8.
5. Wenzhong Y , Shuqun S. Automatic Chromosome Counting Algorithm Based on Mathematical Morphology. Journal of Data Acquis ition and Processing. 2008; 23(9): 1004-9037.
6. Shi .L.Z, Nascimento J.M, Chandsawangbhuwana C, Botvinick EL , Berns MW. An automatic system to study sperm motility and energetics. Biomedical Microdevices. 2008 Aug ; 10(4): 573-83.
7. Abbiramy V, Shanthi V , Allidurai C, Spermatozoa Detection. Countingand Tracking in Video Streams to Detect Asthenozoospermia. International Conference on Signal and Image Processing. 2010; 265-70.
8. Zheng L , Wang Y. The sperm video segmentation based on dynamic threshold. International Conference on Machine Learning and Cybernetics (ICMLC) . 2010.
9. Alias M.F, Isa N.A.M, Sulaiman S.A , Zamli K.Z. Detection of Sprague Dawley Sperm Using Matching Method. Knowledge-Based.Intelligent. Information and Engineering Systems; Berlin, Germany. 2008; 5719(3): 541-7.
10. Abbiramy V.S , Shanthi V, Spermatozoa. Segmentation and Morphological Parameter Analysis Based Detection of Teratozoospermia. International Journal Computer Applications. 2010; 3(7): 19-23.
11. Garcia-Olalla O, Alegre E, Fernandez-Robles L, Malm P, Bengtsson E. Acrosome integrity assessment of boar spermatozoa images using an early fusion of texture and contour descriptors. Computer Methods Programs in Biomedicine. 2015;120(1) :49-64.
12. Bijar A, Mikaeili M, Khayati R , Benavent AP. Fully automatic identification and discrimination of sperm parts in microoscpic images of stained human semen smear. Journal Biomedical Science and Engineering. 2012; 5: 384-95.
13. Chang V, Saavedra JM, Castaneda V, Sarabia L, Hitschfeld N, Hartel S. Gold-standard and improved framework for sperm head segmentation. Computer Methods Programs in Biomedicine. 2014; 117(2): 225-37.
14. Hidayatullah P , Zuhdi M. Automatic sperms counting using adaptive local threshold and ellipse detection.
15. International Conference on Information Technology Systems and Innovation (ICITSI). Bandung-Bail. 2014: 24-7.
16. JiaqIan L, Kuo-Kun, Haiting D , Yifan L. Human Sperm Health Diagnosis with Principal Component Analysis and K-nearest Neighbor Algorithm. Proc International Conference on Medical Biometrics. 2014; 108-13.
17. Tseng TT, Li Y, Hsu C.Y, Huang H.N, Zhao M , Ding M. Computer-Assisted System with Multiple Feature Fused Support Vector Machine for Sperm Morphology Diagnosis. Biomed Research International. 2013; 2013.
18. Chun Tan W , Mat Isa N.A. Segmentation and Detection of Human Spermatozoa using Modified Pulse Coupled Neural Network optimized by Particle Swarm Optimization with Mutual Information. IEEE 10th Conference on Industrial Electronics and Applications (ICIEA); 2015.
19. Shojaedini SV, Kermani A , Nafisi V.R. A New Method for Sperm Detection in Human Semen: Combination of Hypothesis Testing and Local Mapping of Wavelet Sub-Bands. Iranian Journal of Medical Physics. 2012; 9(4): 283-92.
20. Shojaedini SV. A New Method for Sperms Detection in Microscopic Images By Using Fuzzy-Based Decision. 11th Iranian Conference on Medical Physics, Tehran, Iran. 2014.
21. Shojaedini SV , Heydari M. A New Method for Sperm Detection in Infertility Cure: Hypothesis Testing Based on Fuzzy Entropy Decision. Journal of Electrical and Computer Engineering Innovations. 2014; 2(2): 69-76.
22. Shojaedini SV , Heydari M. Automatic Sperm Analysis in Microscopic Images of Human Semen: Segmentation Using Minimization of Information Distance. Iranian Journal of Medical Physics. 2014; 11: 284-93.
23. Shojaedini SV , Heydari M. A New Method for Sperm Characterization for Infertility Treatment: .Hypothesis Testing by Using Combination of Watershed Segmentation and Graph Theory. Journal of medical signals and sensors. 2014; 4(4): 274-80.
24. Shojaedini SV , Parcham K. A New Method for Detecting Sperms in Microscopy Images by Using Combination of Contours and Morphological Processing. 2nd International Conference on Knowledge-Based Research in Computer. Engineering and Information Technology ,Tehran, Iran. 2016.
25. Shojaedini SV, Goldar AR , Soori M. Correntropy based sperm detection: a novel spatiotemporal processing for analyzing videos of human semen. Health and Technology. 2017; 1-8.
26. Haralick RM, Shapiro LG. Computer and Robot Vision. Addison-Wesley Longman Publishing Company, Inc. Boston. 1992; 28-48.
27. Maryellen LG, et al. Automated breast ultrasound in breast cancer screening of women with dense breasts: reader study of mammography-negative and mammography-positive cancers. American Journal of Roentgenology. 2016; 206(6): 1341-50.